

# Differential expression of wild-type and mutant NMMHC-IIA polypeptides in blood cells suggests cell-specific regulation mechanisms in *MYH9* disorders

Shinji Kunishima,<sup>1</sup> Motohiro Hamaguchi,<sup>1</sup> and Hidehiko Saito<sup>2</sup>

<sup>1</sup>Department of Hemostasis and Thrombosis, Clinical Research Center, National Hospital Organization Nagoya Medical Center, Nagoya; and <sup>2</sup>Nagoya Central Hospital, Nagoya, Japan

***MYH9* disorders such as May-Hegglin anomaly are characterized by macrothrombocytopenia and cytoplasmic granulocyte inclusion bodies that result from mutations in *MYH9*, the gene for nonmuscle myosin heavy chain-IIA (NMMHC-IIA). We examined the expression of mutant NMMHC-IIA polypeptide in peripheral blood cells from patients with *MYH9* 5770delG and 5818delG mutations. A specific antibody to mutant NMMHC-IIA (NT629) was raised against the abnormal carboxyl-terminal residues generated by 5818delG. NT629 reacted to recombinant**

**5818delG NMMHC-IIA but not to wild-type NMMHC-IIA, and did not recognize any cellular components of normal peripheral blood cells. Immunofluorescence and immunoblotting revealed that mutant NMMHC-IIA was present and sequestered only in inclusion bodies within neutrophils, diffusely distributed throughout lymphocyte cytoplasm, sparsely localized on a diffuse cytoplasmic background in monocytes, and uniformly distributed at diminished levels only in large platelets. Mutant NMMHC-IIA did not translocate to lamellipodia in surface activated**

**platelets. Wild-type NMMHC-IIA was homogeneously distributed among megakaryocytes derived from the peripheral blood CD34<sup>+</sup> cells of patients, but coarse mutant NMMHC-IIA was heterogeneously scattered without abnormal aggregates in the cytoplasm. We show the differential expression of mutant NMMHC-IIA and postulate that cell-specific regulation mechanisms function in *MYH9* disorders. (Blood. 2008;111:3015-3023)**

© 2008 by The American Society of Hematology

## Introduction

*MYH9* disorders are autosomal dominant macrothrombocytopenias characterized by giant platelets, thrombocytopenia, and Döhle body–like inclusion bodies in the cytoplasm of granulocytes.<sup>1-3</sup> These disorders are caused by heterozygous mutations in *MYH9*, which encodes nonmuscle myosin heavy chain-IIA (NMMHC-IIA), and include the May-Hegglin anomaly, Sebastian, Fechtner, and Epstein syndromes, Alport-like syndrome with macrothrombocytopenia, and nonsyndromic deafness (DFNA17).<sup>4-6</sup> An *MYH9* mutation is always associated with macrothrombocytopenia and granulocyte inclusion bodies from birth, but it does not predict the development of Alport manifestations, including nephritis, deafness, and cataracts. A mutation of *MYH9* alone does not seem to cause associated Alport manifestations, and unknown genetic and/or epigenetic factors might influence the phenotypic consequences of *MYH9* mutations.<sup>7-10</sup> Although the molecular mechanisms of hematologic abnormalities are under investigation, those of the kidney, cochlea, and lens are completely unknown.

We previously showed that NMMHC-IIA polypeptide accumulates in neutrophil cytoplasm and forms inclusion bodies in patients with *MYH9* disorders. The nature of the cytoplasmic accumulation can be classified according to the number, size, and shape of accumulated NMMHC-IIA granules, into types I, II, and III. Type I comprises 1 or 2 large (0.5-2  $\mu\text{m}$ ), intensely stained, oval- to spindle-shaped cytoplasmic NMMHC-IIA–positive granules. Type II comprises up to 20 circular to oval cytoplasmic spots ( $\leq 1 \mu\text{m}$ ). Type III appears as speckled staining. Furthermore, the pattern of localization correlates with the site of *MYH9* mutation. Mutations

in exon 38 and 40 are strictly associated with type I localization and those in exons 16, 26, and 30 are associated with type II localization.<sup>11</sup> Thus the different *MYH9* mutations result in different influences on the assembly of mutant NMMHC-IIA polypeptides. Given that myosin consists of 2 heavy chains and the wild-type NMMHC-IIA molecules are contained in inclusion bodies, the nature of the disease at the molecular level is apparently dominant negative. Although inclusion bodies might be derived as a result of mutant molecules, these conclusions were deduced from indirect observations using antibodies that recognized only wild-type NMMHC-IIA. Recent findings have suggested a haploinsufficiency effect in platelets and megakaryocytes.<sup>12,13</sup> Inclusion bodies are undetectable in lymphocytes, and their presence in monocytes remains controversial. Accordingly, whether mutant NMMHC-IIA is expressed in these cells is obscure.<sup>1,2,14-16</sup> We demonstrated cell-specific mutant NMMHC-IIA expression in *MYH9* disorders for the first time using a specific antibody against mutant NMMHC-IIA.

## Methods

### Patients

We performed *MYH9* mutational analysis on 4 patients with a heterozygous one-base deletion mutation in exon 40 (Table 1) as described.<sup>9</sup> All of the patients had moderate-to-severe thrombocytopenia, but none had a bleeding tendency. Patient 2 and the father of patient 1 who also had an *MYH9*

Submitted October 15, 2007; accepted January 1, 2008. Prepublished online as *Blood* First Edition paper, January 11, 2008; DOI 10.1182/blood-2007-10-116194.

The publication costs of this article were defrayed in part by page charge

payment. Therefore, and solely to indicate this fact, this article is hereby marked "advertisement" in accordance with 18 USC section 1734.

© 2008 by The American Society of Hematology

**Table 1. Clinical and hematologic characteristics of the 4 patients with *MYH9* disorders**

Patient no.	Sex/age, y	Platelet count,* '10/L	Platelet size, $\mu\text{m}$ ,† mean $\pm$ SD	<i>MYH9</i> mutations	Reference
1	M/1	88	5.6 $\pm$ 1.6	5770delG	This study
2	F/36	68	5.2 $\pm$ 1.8	5818delG	Mother of patients 3 and 4
3	M/10	68	5.7 $\pm$ 2.3	5818delG	Kunishima et al <sup>9,11</sup>
4	M/4	40	5.1 $\pm$ 1.5	5818delG	Brother of patient 3

All 4 patients had leukocyte inclusion bodies and type I NMMHC-IIA localization. None of the patients had nephritis, hearing loss, or cataracts.

\*Platelet count was determined manually in a hemocytometer or on peripheral blood smears.

†Platelet size was determined as platelet diameter by microscopic observation of 200 platelets on stained peripheral blood smears (normal control, 2.5  $\pm$  0.3  $\mu\text{m}$ ; n=31).

mutation had been diagnosed with idiopathic thrombocytopenic purpura and treated accordingly. In some experiments, peripheral blood smears from patients with E1841K and a patient with somatic mosaicism for 5818delG were analyzed.<sup>17</sup> Peripheral blood samples were collected after the patients and/or their parents gave informed consent in accordance with the Declaration of Helsinki to participate in the study, which was approved by the ethics review committees at Nagoya Medical Center and at each of the hospitals where the patients were followed up. Immunofluorescence staining, immunoblotting, and quantitative fluorescent polymerase chain reaction (PCR) of peripheral blood samples were analyzed in all of the 4 patients, while analysis of megakaryocytes cultured from CD34<sup>+</sup> peripheral blood cells was performed in patients 2, 3, and 4.

### Antibodies

We raised an antimitant NMMHC-IIA antibody (NT629) against 6 abnormal amino acid residues generated by the 5818delG mutation (Figure 1A). Rats were immunized with synthetic peptides (CKGAGM<sup>AP</sup>TKR; linker cysteine and the normal sequence are underlined) conjugated with keyhole-limpet hemocyanin as a hapten carrier. Antiserum was collected, absorbed with corresponding wild-type peptides (CKGAGDGS<sup>DEE</sup>) followed by human platelet myosin purified from outdated platelet concentrates,<sup>18</sup> and then affinity-purified by chromatography on immobilized antigen peptides. Other antibodies included anti-NMMHC-IIA C-terminal peptide (GKADGAEAKPAE) polyclonal antibody PRB440P (BabCO, Richmond, CA), anti-GPIIb monoclonal antibody SZ22, fluorescein isothiocyanate (FITC)-conjugated anti-GPIIIa antibody SZ21, phycoerythrin (PE)-conjugated anti-GPIIb antibody SZ2 (Immunotech SA, Marseille, France), anti-GPIIb polyclonal antibody, antiactin antibody (Santa Cruz Biotechnology, Santa Cruz, CA), anti- $\alpha$ -tubulin antibody DM1A (Abcam, Cambridge, United Kingdom), anti-myc-tag rabbit polyclonal antibody (Medical and Biological Laboratories, Nagoya, Japan), and anti-myc-tag mouse monoclonal antibody (Invitrogen, San Diego, CA).

### Expression of NMMHC-IIA rod

Lymphocyte mRNA was extracted from patient 2 using a QuickPrep Micro mRNA Purification Kit (GE Healthcare, Little Chalfont, United Kingdom), and first-strand cDNA was synthesized using SensiScript reverse transcriptase and oligo-dT primer (Qiagen, Hilden, Germany). *MYH9* rod sequences (nt 4016-6118 of GenBank no. NM002473) corresponding to light meromyosin (wild-type allele, 1278-1960 aa; 5818delG mutant allele, 1278-1946 aa) were amplified from the cDNA containing the wild-type and mutant sequences using LA Taq DNA polymerase (Takara Bio, Otsu, Japan) and cloned into the pCR2.1Topo vector (Invitrogen). We introduced a myc epitope tag fused at the 5' end to *MYH9* cDNA using inverse PCR mutagenesis.<sup>19</sup> Oligonucleotide primers were designed in inverted tail-to-tail directions to amplify the wild-type and 5818delG *MYH9*/pCR2.1Topo construct. PCR amplification proceeded with a forward primer (5'-CTGCAGGTGGAGCTGGACAACGTGACC-3') and a mutagenic reverse primer, which included a myc-tag-coding sequence (5'-CAGATCCTCTCTCTGAGATGAGTTTTTGTTCATACCAAGCTTGGC-3'; myc-tag-coding sequence is underlined) with LA Taq DNA polymerase. Amplified DNA fragments were self-ligated with T4 polynucleotide kinase and T4 ligase (Promega, Madison, WI), and used to transform DH5 $\alpha$  competent cells. The recovered plasmids were sequenced, and each insert containing myc-*MYH9* cDNA was excised with *HindIII/NotI* and shuttled into the

mammalian expression vector, pCDNA3.1 (Invitrogen). All constructs were confirmed by restriction analysis and sequencing.

The pCDNA3.1 vector containing either the myc-tagged wild-type rod *MYH9* cDNA or 5818delG rod *MYH9* cDNA was transiently transfected into 293T cells. Briefly, 10<sup>5</sup> 293T cells were seeded in 35-mm dishes and incubated overnight. Plasmid DNA (1.0  $\mu\text{g}$ ) was then transfected into the cells using Polyfect transfection reagent (Qiagen) according to the manufacturer's instructions. Cytospin preparations were analyzed by immunofluorescence staining, and whole cell extracts were immunoblotted 24 hours later.

### Fractionation of peripheral blood cells

Neutrophils, platelets, monocytes, and lymphocytes were isolated from peripheral blood collected into acid-citrate-dextrose. After erythrocyte sedimentation using dextran, supernatants were centrifuged on Ficoll-Paque (GE Healthcare) at 400g for 30 minutes. Platelet-rich plasma prepared from the intermediate mononuclear cell fraction by centrifugation at 100g for 10 minutes was passed through a leukocyte reduction filter (Terumo, Tokyo, Japan). Platelets were washed once, resuspended in Hanks balanced salt solution (Invitrogen) containing 2 mM ethylenediaminetetraacetic acid (EDTA) and 0.5% bovine serum albumin, and then incubated with anti-CD61 antibody conjugated to magnetic microbeads (Miltenyi Biotec, Bergisch Gladbach, Germany). CD61<sup>+</sup> cells (platelet fraction) were captured using magnetic separation columns. Monocytes were isolated from the Ficoll-Paque mononuclear cell fraction using anti-CD14 magnetic beads. We isolated lymphocytes by washing the CD14<sup>+</sup> monocyte-depleted pass-through fraction 3 times for 10 minutes each at 100g to remove platelets. Erythrocytes in the Ficoll-Paque pellet were lysed in hypotonic saline to obtain CD16<sup>+</sup> cells (neutrophil fraction). The cells in each fraction were counted using a hemocytometer and purity was evaluated by May-Grünwald-Giemsa staining and microscopy. The final platelet fraction contained no more than 2 leukocytes/10<sup>5</sup> platelets, and monocytes, neutrophils, and lymphocytes were more than 98%, 99%, and 98% pure, respectively.

### Analysis of megakaryocytes from CD34<sup>+</sup> peripheral blood cells

CD34<sup>+</sup> cells (5-10  $\times$  10<sup>3</sup> cells) were isolated from the Ficoll-Paque mononuclear cell fraction of 10 mL peripheral blood using anti-CD34 magnetic beads (Miltenyi Biotec). Cells were cultured in StemSpan Serum-Free Expansion Medium supplemented with 50 ng/mL TPO, 50 ng/mL SCF, and 10 ng/mL IL3 (Stem Cell Technologies, Vancouver, BC) in a humidified atmosphere of 5% CO<sub>2</sub> for 12 days. Culture supernatants obtained after low-speed centrifugation (100g for 8 minutes) were analyzed by 2-color flow cytometry using FITC-conjugated anti-GPIIIa antibody SZ21 and PE-conjugated anti-GPIIb antibody SZ2. Cytospin preparations of cultured megakaryocytes were analyzed by immunofluorescence staining.

### Quantitative fluorescent PCR analysis

Normal and mutant alleles were amplified by quantitative fluorescent PCR that discriminated a one-nucleotide difference in each PCR product.<sup>17</sup> Total RNA was extracted from platelets, neutrophils, monocytes, and lymphocytes using a NucleoSpin RNA/Protein kit (Macherey-Nagel, Düren, Germany), and first-strand cDNA was synthesized using SensiScript reverse transcriptase and an oligo-dT primer (Qiagen). Primers 395 (5'-ATGCCATGAACCGC-GAAGTC-3') and 6-FAM-labeled 4035 (5'-6-FAM-GGCTTATTCGGCAG-GTTTGG-3') were included in the PCR mixture and amplification proceeded over 35 cycles of 20 seconds at 95°C, 20 seconds at 58°C, and

**A**

**Wild-type**

5770 5818  
 G CGC GGG GAC CTG CCG TTT GTC GTG CCC CGC CGA ATG GCC CGG AAA GGC GCC GGG GAT GGC TCC GAC GAA GAG GTA GAT GGC AAA GCG GAT GGG GCT GAG GCC AAA CCT GCC GAA TAA  
 R G D L P F V V P R R M A R K G A G D G S D E E V D G K A D G A E A K P A E \*

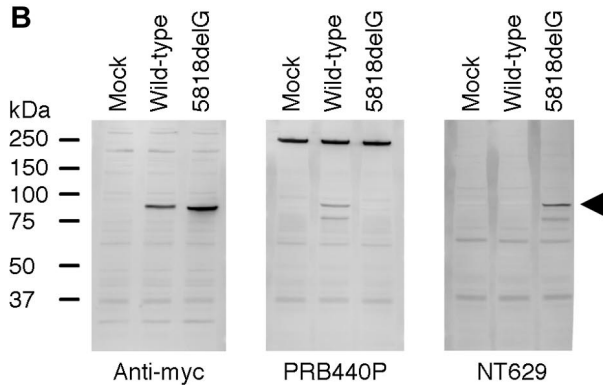
**5770delG**

G CGC GGG ACC TGC CGT TTG TCG TGC CCC GCC GAA TGG CCC GGA AAG GCG CCG GGG ATG GCT CCG ACG AAG AGG TAG  
 R G **T** C R L S C P A E W P G K A P G M A P T K R \*

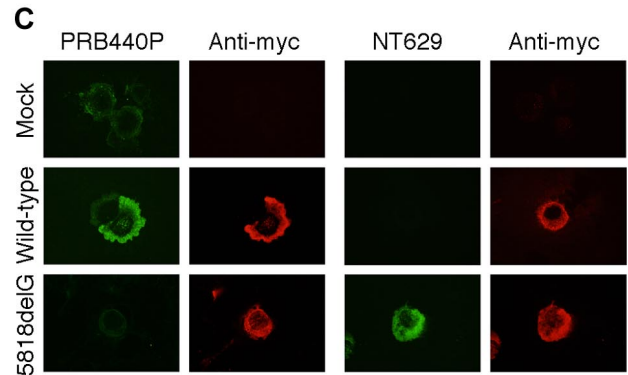
**5818delG**

G CGC GGG GAC CTG CCG TTT GTC GTG CCC CGC CGA ATG GCC CGG AAA GGC GCC GGG ATG GCT CCG ACG AAG AGG TAG  
 R G D L P F V V P R R M A R K G A G M A P T K R \*

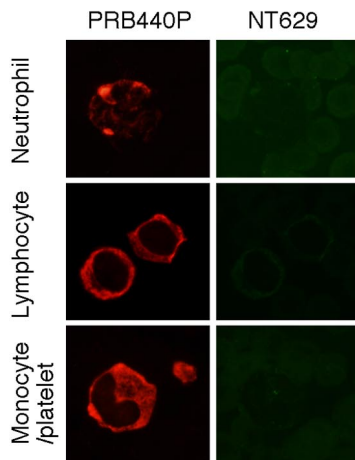
**B**



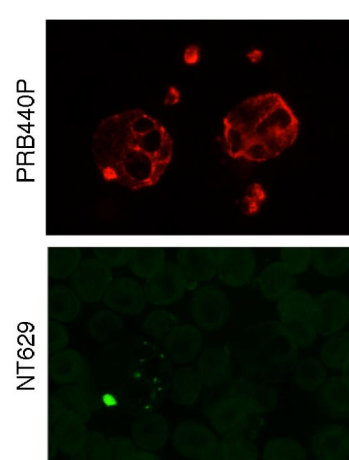
**C**



**D**



**E**



**F**

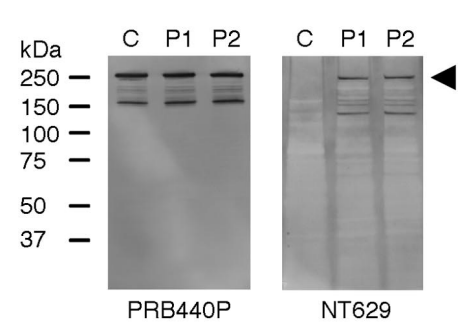
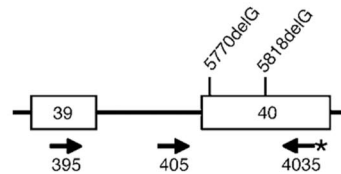


**Figure 1. Characterization of NT629 antibody.** (A) Site of single nucleotide deletions in *MYH9* exon 40 and amino acid sequence of NMMHC-IIA carboxyl-terminal region. Nucleotides encoding amino acids are numbered beginning with initiation codon. Deduced amino acid sequence is written under nucleotide sequence. Deletions of a single guanine nucleotide (bold type) results in frameshift that cause replacement by aberrant amino acids at the carboxyl terminus (bold type) and premature termination. Epitopes of PRB440P and NT629 antibodies are underlined. (B) Total proteins of 293T cells transiently transfected with vectors expressing N-terminal myc-tagged wild-type *MYH9* rod (1278-1960 aa) and 5818delG mutant *MYH9* rod (1278-1946 aa) were analyzed by immunoblotting. Band corresponding to recombinant myc-tagged NMMHC-IIA rod was detected with antimyc antibody in both wild-type *MYH9*- and 5818delG *MYH9*-transfected cells. PRB440P and NT629 detected recombinant NMMHC-IIA rod only in wild-type *MYH9*-transfected cells and in 5818delG *MYH9*-transfected cells (arrow head), respectively. Endogenous 220-kDa NMMHC-IIA band was detected in 293T cells with PRB440P. (C) Immunofluorescence analysis of 293T cells transiently transfected with N-terminal myc-tagged wild-type *MYH9* rod and 5818delG *MYH9* rod expression vectors double stained with PRB440P and antimyc mouse antibody, and with NT629 and antimyc rabbit antibody, respectively. PRB440P and NT629 intensely stained cytoplasm only in wild-type- and only in 5818delG-transfected cells, respectively. PRB440P weakly stained endogenous NMMHC-IIA in nontransduced 293T cells. (D) Immunofluorescence analysis of peripheral blood smears from a patient with E1841K double stained with PRB440P and NT629. PRB440P showed abnormal type I NMMHC-IIA localization in all neutrophils with diffusely stained background, and diffuse cytoplasmic staining in lymphocytes, monocytes, and platelets. In contrast, cells were not stained with NT629 antibody. (E) Immunofluorescence analysis of peripheral blood smears from a mosaic patient for 5818delG double-stained with PRB440P and NT629. PRB440P showed abnormal type I NMMHC-IIA localization in approximately 10% neutrophils, in which inclusion bodies were stained with NT629. Normal neutrophils with diffuse NMMHC-IIA distribution were not stained with NT629. (F) Immunoblots of buffy coat samples from healthy control and from patients 1 (5770delG) and 2 (5818delG). NT629 detected band corresponding to NMMHC-IIA polypeptide and additional small band in blood from patients, but not control.

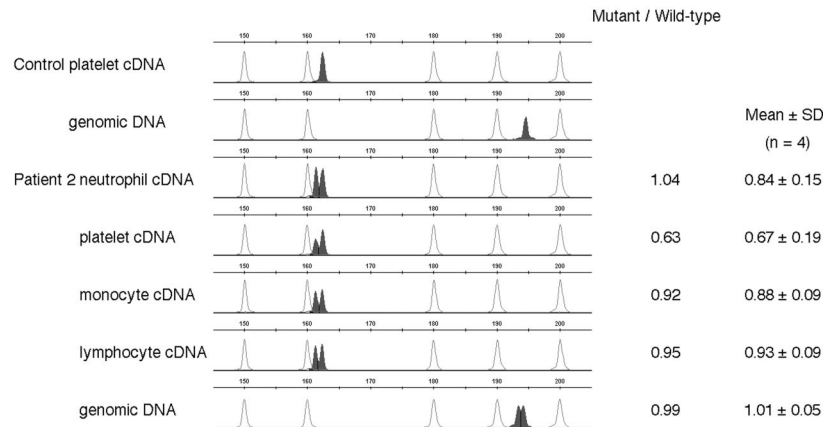
20 seconds at 72°C using AmpliTaq Gold DNA polymerase (Applied Biosystems, Foster City, CA). For comparison, fluorescent PCR was also performed on genomic DNA extracted using QIAamp Tissue Kits (Qiagen), using primers 405 (5'-TTGAGATGTGGCTGTGC-3')

and 6-FAM-labeled 4035. The PCR products were examined using an ABI 310 Genetic Analyzer and data were analyzed using GeneMapper 3.7 software (Applied Biosystems). Peak areas of normal and mutant alleles were calculated for each sample.

A



B



### Immunofluorescence analysis

Peripheral blood smears were analyzed by immunofluorescence staining as described.<sup>11</sup> In brief, EDTA-anticoagulated peripheral blood samples were smeared on glass slides, air-dried, fixed in methanol, permeabilized with acetone, hydrated, and blocked with normal goat serum. The slides were concomitantly incubated with PRB440P and NT629 and then reacted with Alexa 555-labeled anti-rabbit IgG and Alexa 488-labeled anti-rat IgG (Invitrogen). Megakaryocytes derived from CD34<sup>+</sup> peripheral blood cells and 293T cells transfected with the myc-tagged *MYH9*/pcDNA3.1 were simultaneously analyzed. Stained cells were examined using a BX50 fluorescence microscope with a 100×/1.35 numeric aperture oil objective (Olympus, Tokyo, Japan). Images of the slides were acquired using a DP70 digital camera and DP Manager software (Olympus).

### Immunoblotting

Protein samples were simultaneously isolated with total RNA using NucleoSpin RNA/Protein kits, separated by sodium dodecyl sulfate-polyacrylamide gel electrophoresis (SDS-PAGE) on 4 to 12% gradient acrylamide slab gels (Invitrogen) under reduced conditions, and electroblotted onto polyvinylidene difluoride membranes (Bio-Rad Labs, Hercules, CA). The blots were cut horizontally in half at the approximate position of the 75-kDa molecular marker. The upper half of each blot was probed with PRB440P or NT629, and the lower portions were reacted with antiactin antibody followed by horseradish peroxidase-conjugated secondary antibody. The bound antibodies were visualized using an enhanced chemiluminescent substrate. Signal ratios of NT629 to PRB440P were determined densitometrically on immunoblot images using National Institutes of Health ImageJ software (<http://rsb.info.nih.gov/ij/>, Bethesda, MD). Total expression of the myc-tagged NMMHC-IIA polypeptide in the transfected cells was also analyzed using antimyc antibody PRB440P or NT629.

## Results

### Mutant *MYH9* mRNA is expressed in peripheral blood cells, at lower levels in platelets

Deutsch et al have found normal amounts of mutant *MYH9* mRNA in the total peripheral blood cells of patients with *MYH9* disorder.<sup>12</sup>

We further investigated mutant *MYH9* expression in fractionated blood cells. We simultaneously amplified wild-type and mutant alleles and discriminated alleles differing by one nucleotide using quantitative fluorescent PCR (Figure 2A). The signal ratio of mutant to wild-type alleles in genomic DNA samples from the 4 patients was 1.01 (± 0.05), demonstrating equal amplification efficiency of wild-type and mutant alleles. The results obtained with cDNAs from isolated neutrophils, lymphocytes, and monocytes were the same, indicating normal mutant *MYH9* expression. In contrast, the signal ratio in platelets was moderately decreased to 0.67 (± 0.19, n = 4; Figure 2B).

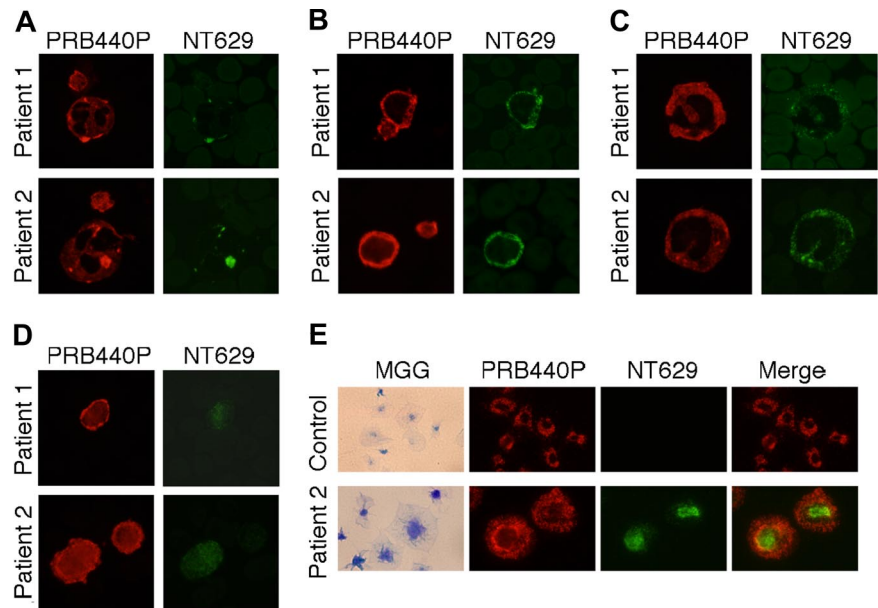
### Characterization of antimutant NMMHC-IIA antibody specific for abnormal C-terminal amino acids generated by 5818delG

To specifically detect mutant NMMHC-IIA polypeptide and explore its subcellular localization, we developed the rat polyclonal antibody NT629 that reacts to the unique abnormal C-terminal peptide generated by 5818delG. Figure 1A shows that any exon 40 one-base nucleotide deletion located 5' to nt 5818 resulted in a frameshift and generated the abnormal C-terminal MAPTKR sequence before premature termination. Accordingly, the antigenic sequence is maintained in the 5770delG mutant. An enzyme-linked immunosorbent assay showed that affinity-purified NT629 reacted to immobilized immunogenic peptides but not to corresponding wild-type peptides (data not shown). Immunofluorescence and immunoblot analyses of 293T cells expressing recombinant NMMHC-IIA rod and peripheral blood samples were performed to validate the specificity of NT629.

We transiently transfected 293T cells with the N-terminal myc-tagged wild-type and 5818delG mutant *MYH9* rod constructs. An approximately 80-kDa band, which is consistent with the calculated molecular weight of the recombinant wild-type (79.0 kDa) and of 5818delG (77.7 kDa) NMMHC-IIA rod, was detected in total proteins of 293T cells expressing recombinant NMMHC-IIA rod that were immunoblotted with anti-myc-tag antibody (Figure 1B left panel). Probing the blots with PRB440P revealed the

**Figure 2. Mutant *MYH9* mRNA is expressed in peripheral blood cells, but to a lesser extent in platelets.** (A) Genomic map of *MYH9* exon 39 and 40 region and locations of primers (arrows) used for quantitative fluorescent PCR amplification. PCR was performed on cDNA samples from neutrophils, platelets, monocytes, and lymphocytes using primers 395 and 6-FAM-labeled 4035. Genomic DNA was also amplified by fluorescent PCR using primers 405 and 6-FAM-labeled 4035 for comparison. PCR products were examined using an ABI 310 Genetic Analyzer and data were analyzed. Boxes (numbered) and lines represent exons and introns, respectively, and are not drawn to scale. (B) Representative electropherograms of fluorescent PCR products from patient 2 with *MYH9* 5818delG. Signal ratios of mutant allele (161-bp peak) to wild-type allele (162-bp peak) are shown at right of each trace. Mean signal ratio of 4 patients is shown at far right. Ratio is approximately 0.9 in neutrophils, monocytes, and lymphocytes, but moderately decreased in platelets.

**Figure 3. Differential expression of mutant NMMHC-IIA polypeptide in peripheral blood cells.** Immunofluorescence analysis of peripheral blood smears from patients 1 and 2 double stained with PRB440P (red) and NT629 (green). (A) PRB440P stained granular NMMHC-IIA accumulation and diffusely stained cytoplasm of neutrophils, whereas NT629 stained only intense cytoplasmic foci and no background. (B) Lymphocytes were diffusely stained with both PRB440P and NT629. (C) In monocytes, both PRB440P and NT629 detected small dots in addition to diffuse cytoplasmic staining. Platelets in panels A-B are notably not stained with NT629. (D) PRB440P diffusely stained platelet cytoplasm and intensely stained cell periphery. In contrast, most platelets are NT629 negative; only extraordinarily large platelets are diffusely stained. (E) Mutant NMMHC-IIA polypeptide cannot translocate to lamellipodia in surface-activated platelets. Platelets were adhered to glass slides for 10 minutes, fixed, and processed for PRB440P and NT629 immunofluorescence analysis. Left column: images stained with May-Grünwald-Giemsa. Mutant NMMHC-IIA was weakly distributed only in granulomere zone of platelets from patients. Platelets from patients 2, 3, and 4 were examined. Original magnification,  $\times 1000$ .



approximately 80-kDa band only in the wild-type. An endogenous NMMHC-IIA of the 220-kDa band was detected in mock-, wild-type-, and 5818delG-transfected 293T cells (Figure 1B middle panel). NT629 revealed only the approximately 80-kDa band in cells transfected with 5818delG (Figure 1B right panel). Immunofluorescence analysis with PRB440P revealed weak cytoplasmic staining in the mock-transfected cells due to the presence of endogenous NMMHC-IIA. Anti-myc-tag antibodies and NT629 were not reactive in these cells. Cytoplasmic staining with PRB440P was intense only in wild-type-transfected cells, and NT629 was intensely stained only in 5818delG-transfected cells. Positive staining with anti-myc-tag antibody and the negative staining with PRB440P and NT629 in the wild-type- and 5818delG-transfected cells, respectively, confirmed that PRB440P and NT629 did not recognize 5818delG and wild-type NMMHC-IIA rod, respectively (Figure 1C).

We concomitantly stained conventional peripheral blood smears with PRB440P and NT629. PRB440P diffusely stained granulocytes, platelets, lymphocytes, and monocytes, whereas NT629 reactivity was absent in control smears (data not shown). PRB440P detected abnormal type I NMMHC-IIA in all neutrophils with a diffusely stained background from patients with *MYH9* E1841K, but NT629 did not react to inclusion bodies, indicating that NT629 does not react to E1841K mutant NMMHC-IIA aggregates (Figure 1D). We analyzed blood smears from a patient with somatic mosaicism for the *MYH9* 5818delG to reconfirm the specificity of NT629. Figure 1E shows that PRB440P detected morphologically normal neutrophils and neutrophils containing inclusion bodies ( $\sim 10\%$  of total neutrophils), whereas NT629 reacted to the inclusion bodies but not to normal neutrophils.

To further verify the specificity of NT629, buffy coat samples from a healthy control and from patients 1 and 2 were immunoblotted (Figure 1F). NT629 detected bands corresponding to NMMHC-IIA polypeptide and an additional small band in the patients, but detected none in the healthy control. After NT629 preabsorption with the antigen peptide, the immunofluorescence signal on stained smears and immunoreactive bands on the blots disappeared, confirming that the antibody was specific (data not shown). Thus, NT629 reacted only to NMMHC-IIA due to an *MYH9* exon 40

one-base deletion such as 5770delG and 5818delG and did not recognize any normal cellular components.

#### Mutant NMMHC-IIA polypeptide is sequestered only in inclusion bodies in neutrophils

We applied the NT629 to investigate the expression and localization of mutant NMMHC-IIA on peripheral blood smears from patients with *MYH9* 5770delG (patient 1) and 5818delG (patients 2, 3, and 4; Table 1). Figure 3 shows representative immunofluorescence staining of peripheral blood cells. Immunofluorescence analysis of neutrophil NMMHC-IIA with PRB440P disclosed the type I pattern containing 1 or 2 large, intensely stained, oval- to spindle-shaped cytoplasmic NMMHC-IIA-positive granules.<sup>11</sup> In addition to bright foci, PRB440P diffusely stained the cytoplasm, indicating that wild-type NMMHC-IIA accumulates in inclusion bodies and that residual amounts are distributed outside such structures. In contrast, NT629 intensely stained foci, but not the background in the same neutrophils, indicating that mutant NMMHC-IIA is sequestered and localized only in inclusion bodies (Figure 3A).

#### Mutant NMMHC-IIA polypeptide is diffusely distributed in lymphocyte cytoplasm, and sparsely localized on a diffuse cytoplasmic background in monocytes

Inclusion bodies are absent in lymphocytes.<sup>1,2</sup> We previously showed diffuse NMMHC-IIA distribution in lymphocytes from patients with *MYH9* disorders.<sup>5,11</sup> We found that both wild-type and mutant NMMHC-IIA were diffusely distributed in the lymphocyte cytoplasm (Figure 3B). Although the original report of May-Hegglin anomaly described that inclusion bodies are absent in monocytes, this remains controversial.<sup>1,2,14-16</sup> We detected small punctuate foci on a diffuse cytoplasmic background using both PRB440P and NT629 in some monocytes, although the foci were smaller than those observed in neutrophils (Figure 3C). This indicated that some mutant NMMHC-IIA accumulated in definite structures and the remainder does not accumulate or aggregate but distributes outside such structures in monocytes.

### Mutant NMMHC-IIA polypeptide is uniformly distributed at lower levels only in large platelets

The staining profiles of PRB440P and NT629 in platelets from patients were quite different. NMMHC-IIA is homogeneously distributed in the cytoplasm of normal resting platelets.<sup>5,11,20,21</sup> PRB440P diffusely stained the cytoplasm of platelets from the patients, and intensely stained the cell periphery (Figure 3A,B left panels). In contrast, most platelets were negative for NT629 staining (Figure 3A,B right panels) and only those that were similar to or larger than erythrocytes (~10% of total platelets) were weakly stained in the cytoplasm but not in the cell periphery (Figure 3D). Although mutant NMMHC-IIA expression was remarkably decreased, it did not accumulate or aggregate to form inclusion bodies, and remained uniformly distributed in the cytoplasm.

The distribution profiles of wild-type and mutant NMMHC-IIA were more distinct in surface-activated platelets (Figure 3E). When platelets are activated on glass slides for 10 minutes, they change shape from discoid to spherical, extend filopodia and lamellipodia, and spread with large circumferential lamellae. Immunofluorescence analysis revealed the mutually exclusive localization of wild-type and mutant NMMHC-IIA. NMMHC-IIA was distributed in a discrete granular pattern in the cell body but not in the central granule zone of normal platelets. Wild-type NMMHC-IIA was normally distributed in the cell body and weakly in the granule zone of platelets from patients 2, 3, and 4. However, mutant NMMHC-IIA detected by NT629 was weakly distributed only in the granule (the images are bright, but they were acquired over a long exposure time). These results indicated that upon surface activation, wild-type NMMHC-IIA reorganized, whereas mutant NMMHC-IIA was unable to translocate to lamellipodia. In addition, residual wild-type NMMHC-IIA localization in the granule zone, which was undetectable in control platelets, might result from wild-type and mutant NMMHC-IIA association.

The decreased expression of mutant NMMHC-IIA in platelets was consistent with the results of immunoblotting, in which the relative amount of mutant NMMHC-IIA was more decreased than in leukocytes. Densitometric quantitation showed that the signal ratios of NT629 to PRB440P were  $0.41 (\pm 0.10)$ ,  $0.26 (\pm 0.06)$ ,  $0.40 (\pm 0.17)$ , and  $0.04 (\pm 0.01)$ ;  $n = 3$ ) in neutrophils, monocytes, lymphocytes, and platelets, respectively (Figure 4).

### Mutant NMMHC-IIA polypeptide is heterogeneously distributed in megakaryocytes

We examined mutant NMMHC-IIA expression in platelet precursor megakaryocytes. Because bone marrow specimens could not be obtained from the patients, CD34<sup>+</sup> cells derived from peripheral blood were cultured in liquid serum-free medium supplemented with a cocktail of cytokines to induce megakaryocyte differentiation. Twelve days later, cultured megakaryocytes were identified by cell morphology (large cells with multilobulated nuclei and abundant cytoplasm) and the expression of GPIIb or von Willebrand factor on cytospin preparations. NMMHC-IIA expression was analyzed by double staining with anti-GPIIb and PRB440P or NT629. NMMHC-IIA was homogeneously distributed in the cytoplasm of normal megakaryocytes (Figure 5A top panels). Although wild-type NMMHC-IIA was normally distributed in megakaryocytes from patients, mutant NMMHC-IIA was coarse and heterogeneously distributed (Figure 5A top and bottom panels). The limited numbers of megakaryocytes derived from peripheral blood CD34<sup>+</sup> cells caused difficulties when trying to

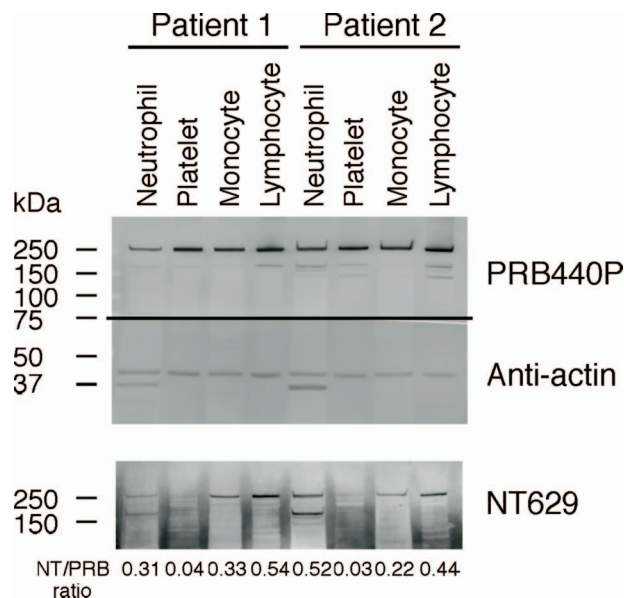


**Figure 4. Mutant NMMHC-IIA polypeptide is present in leukocytes but decreased in platelets.** Immunoblot analysis of isolated neutrophils, platelets, monocytes, and lymphocytes from patients 1 and 2. Whole cell proteins were separated by SDS-PAGE and resolved proteins were electroblotted onto polyvinylidene difluoride membranes. Blots were cut horizontally in half at approximate position of 75-kDa molecular marker. The top half of each blot was probed with PRB440P or NT629; bottom portions were reacted with antiactin antibody. A horizontal line has been inserted to indicate where the gel was cut. Top panels show blots probed with PRB440P and antiactin antibody. Bottom panel shows blots probed with NT629. Analysis with NT629, which recognizes only mutant NMMHC-IIA polypeptide, revealed mutant NMMHC-IIA expression in neutrophils, lymphocytes, and monocytes but obviously decreased expression in platelets. Signal ratio of NT629 to PRB440P is also obviously decreased in platelets compared with leukocytes.

determine the relative levels of mutant NMMHC-IIA by immunoblotting. The percentage of megakaryocytes was less than 10% of cultured cells.

In this culture system, platelet-like particles were released from megakaryocytes. Although no typical proplatelet-forming megakaryocytes were observed, some platelet-producing megakaryocytes were detected on cytospin preparations (Figure 5B). Platelet-like particles derived from the patients were larger than those of healthy controls according to their mean diameters on cytospin preparations (controls vs patients:  $2.6 \pm 0.7$  vs  $6.0 \pm 1.3$   $\mu\text{m}$ ;  $n = 3$  each) or geometric means of forward scatter of GPIIb and GPIIIa double-positive cells determined by flow cytometry (controls vs patients:  $233.0 \pm 1.7$  vs  $294.8 \pm 9.3$ ;  $n = 3$  each; Figure 5C).

## Discussion

We produced a rat polyclonal antibody, NT629, that recognizes the unique abnormal C-terminal peptide generated by 5818delG, and presented the first evidence of mutant NMMHC-IIA polypeptide expression and localization in peripheral blood cells from patients with *MYH9* disorders. We extensively validated the specificity of NT629 through studies of 293T cells expressing recombinant NMMHC-IIA, peripheral blood smears from healthy individuals and patients, and buffy coat extracts. NT629 reacted only with mutant NMMHC-IIA polypeptide generated by an *MYH9* exon 40 one-base deletion such as 5770delG and 5818delG and it did not recognize any normal cellular components.

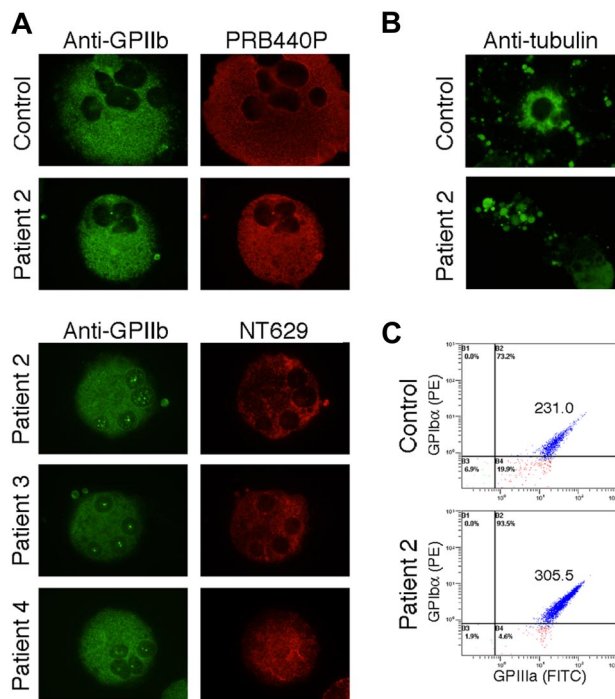


**Figure 5. NMMHC-IIA localization in megakaryocytes derived from peripheral blood CD34<sup>+</sup> cells.** (A) Megakaryocytes derived from peripheral blood CD34<sup>+</sup> cells of healthy controls and patients were double-stained with anti-GPIIb mouse monoclonal antibody SZ22 (green) and PRB440P (red, top panels) or with anti-GPIIb rabbit polyclonal antibody (green) and NT629 (red, bottom panels). PRB440P diffusely stained cytoplasm of megakaryocytes from control and patients, whereas NT629 coarsely and heterogeneously stained those of patients. (B) Megakaryocytes that produce platelets. Original magnification,  $\times 1000$ . (C) Flow cytometric analysis of plateletlike particles double stained with anti-GPIIb $\alpha$  and anti-GPIIIa antibodies. Geometric mean of forward scatter of GPIIb $\alpha$  and GPIIIa double-positive cells was shown in inset.

Concomitant immunofluorescence staining with NT629 and PRB440P antibodies enabled the differential detection of intracellular mutant and wild-type NMMHC-IIA polypeptides. Mutant NMMHC-IIA detected by NT629 was localized only as punctuate or granular structures in the cytoplasm of neutrophils in doubly stained peripheral blood smears. In contrast, wild-type NMMHC-IIA detected by PRB440P was localized as such structures and also diffusely distributed in the cytoplasm. Nonmuscle myosin II assembly involves the dimerization of 2  $\alpha$ -helices to form a coiled-coil rod structure and lateral associations of the coiled-coils to form a functional filament.<sup>22</sup> Since myosin consists of 2 heavy chains, then it should assemble in a cell as a mixture of wild-type homodimers, heterodimers consisting of one mutant and one wild-type molecule, and mutant homodimers. *MYH9* disorders are heterozygous conditions in which one allele contains the mutation. If the expression of the wild-type and mutant NMMHC-IIA is equal and the association occurs randomly, 50% of the myosin molecules should be heterodimers and the remainder should comprise homodimers of the mutant (25%) or the wild-type (25%), and thus 75% of the myosin molecules will contain at least 1 mutant NMMHC-IIA. Mutant myosin molecules might also copolymerize into filaments with wild-type myosin molecules that could impair the function and localization of normal wild-type myosin. This assumption is consistent with the findings of Franke et al, who demonstrated that recombinant NMMHC-IIA rod mutants form aberrant aggregates and form dominant insoluble aggregates in the presence of wild-type NMMHC-IIA.<sup>23</sup> Pecci et al reported that NMMHC-IIA levels in granulocytes from patients with *MYH9* disorders were decreased to 32% of controls.<sup>13</sup> They might have

detected only wild-type NMMHC-IIA by immunoblotting because myosin molecules containing mutant NMMHC-IIA were trapped within inclusion bodies and lost during granulocyte lysate preparation. If so, then 68% would have been myosin-containing mutant NMMHC-IIA instead of the predicted 75%. Taken together, mutant NMMHC-IIA aggregates and accumulates in granulocytes to form cytoplasmic inclusion bodies and thus dominant-negative effects indeed serve as the molecular mechanism underlying the formation of such bodies.

The results of our study provide important insights into the molecular mechanisms underlying the production of giant platelets in *MYH9* disorders. Mutant NMMHC-IIA was expressed at obviously decreased levels only in large platelets. Comparative quantitative analysis was not possible because control samples expressing wild-type and mutant NMMHC-IIA polypeptides cannot be obtained. However, the relative amount of mutant to wild-type NMMHC-IIA expression levels in platelets was approximately 10% of the leukocyte levels. The obviously decreased amount of mutant NMMHC-IIA in platelets predicts that the total NMMHC-IIA content would be reduced to approximately 50% of normal levels. This is exactly what Deutsch et al<sup>12</sup> and Pecci et al<sup>13</sup> found independently in platelets from patients with *MYH9* disorders, namely an approximately 50% reduction of NMMHC-IIA compared with the total actin concentration. In addition, we did not detect aggregation or accumulation of mutant NMMHC-IIA in platelets from patients, which is consistent with the fact that overall NMMHC-IIA localization in platelets from patients with *MYH9* disorders is normal.<sup>11,13</sup> Instead, it was uniformly distributed in the cytoplasm and the localization was distinct from the wild-type molecule. Upon contact with a glass surface, platelets change from a discoid to a spherical shape, extend filopodia, and spread with large sheetlike lamellipodia. Myosin becomes associated with actin and comigrates to the front of the lamellipodia, and associates with the granule zone.<sup>24-26</sup> Biochemical analyses have also shown that activation increases the myosin content in the cytoskeleton.<sup>27,28</sup> Canobbio et al recently reported that the increase in cytoskeletal-associated myosin in activated platelets is impaired in patients with *MYH9* disorders.<sup>29</sup> The most recent findings described by Leon et al demonstrated that megakaryocyte-restricted *MYH9* knockout mice lack platelet contractile phenomena, including clot retraction, platelet shape change, and stress-fiber formation on a fibrinogen-coated surface, whereas the heterozygous knockout mice have no abnormalities.<sup>30</sup> Our results substantiate previous findings that mutant NMMHC-IIA does not translocate to the lamellipodia in surface-activated platelets. We conclude that the overall defect in platelets with mutant NMMHC-IIA is haploinsufficiency. We also propose that only residually expressed mutant myosin has a loss of function and cannot participate in the reorganization of cytoskeletal contractile structures.

The macrothrombocytopenia associated with *MYH9* disorders could be caused by impaired platelet release due to abnormal megakaryocyte fragmentation.<sup>31,32</sup> Recent findings have shown that NMMHC-IIA attenuates proplatelet formation,<sup>33,34</sup> which occurs in terminally mature megakaryocytes where most of the cytoplasm is converted into lengthy beaded extensions.<sup>35</sup> Thus, NMMHC-IIA might restrain thrombopoiesis until megakaryocytes accumulate sufficient quantities of the materials required for optimal platelet assembly; loss of myosin-IIA function could trigger precocious proplatelet formation, whereas gain-of-function mutations might limit platelet production. Consistent with recent findings,<sup>12,13</sup> we found that wild-type NMMHC-IIA localization was normal in megakaryocytes derived from the peripheral blood CD34<sup>+</sup> cells of

patients with *MYH9* disorders. However, the distribution of mutant NMMHC-IIA was coarse and heterogeneous. Although immunofluorescence staining for the first time revealed that mutant NMMHC-IIA is expressed in megakaryocytes, this finding was not quantitative. From this viewpoint, Pecci et al demonstrated from indirect immunoblot findings that mutant NMMHC-IIA is absent and that most or the whole of NMMHC-IIA is wild type in megakaryocytes derived from peripheral blood CD34<sup>+</sup> cells, indicating that *MYH9* mutations result in haploinsufficiency in megakaryocytes.<sup>13</sup> However, simple haploinsufficiency for *MYH9* alone cannot explain the pathogenesis of giant platelets and thrombocytopenia in *MYH9* disorders. Mice heterozygous for *Myh9*-null allele do not exhibit giant platelets and thrombocytopenia.<sup>36,37</sup> Evidence also indicates that different *MYH9* mutations result in different consequences for the platelet phenotype. Patients with *MYH9* mutations in the head domain, especially those at the R702 residue, have significantly larger platelets than those with mutations in the tail domain.<sup>38</sup> These findings indicate that despite decreased expression levels, mutant NMMHC-IIA affects the production of platelets in some manner.

We found that the expression levels of mutant *MYH9* mRNA in leukocytes (neutrophils, lymphocytes, and monocytes) from fractionated peripheral blood were normal. Our results are generally consistent with those of Deutsch et al who reported normal amounts of mutant *MYH9* mRNA in total peripheral blood cells of patients with a D1424N mutation.<sup>12</sup> However, we found moderately decreased levels of mutant *MYH9* mRNA in platelets. Because platelets are anucleated, their mRNA content is a consequence of gene expression in precursor megakaryocytes. Thus, mutant *MYH9* mRNA could be slightly more unstable than wild-type mRNA in platelets, and such a subtle difference was undetectable in leukocytes. Furthermore, since leukocytes contain approximately 12 500-fold more mRNA than platelets, residually contaminated leukocytes could affect mRNA levels in platelets and thus they might be overestimated in platelets.<sup>39</sup>

Inclusion bodies are present in granulocytes but not in lymphocytes in patients with *MYH9* disorders.<sup>1,2</sup> Accordingly, whether mutant NMMHC-IIA is expressed in lymphocytes has remained obscure. The present study discovered that the distribution of mutant NMMHC-IIA in lymphocytes is diffuse. Meanwhile the original report of the May-Hegglin anomaly, the prototype of

macrothrombocytopenia with leukocyte inclusion bodies, described the absence of inclusion bodies in monocytes.<sup>1,2</sup> So far, the presence of inclusion bodies in monocytes remains controversial.<sup>1,2,14-16</sup> Mutant NMMHC-IIA was sparsely localized on a diffuse cytoplasmic background in monocytes. Transcription of *MYH9* is regulated in a cell type-specific manner and by its differentiation stage, and differential translational mechanisms are also suggested.<sup>40</sup> Although the mechanisms of how considerable amounts of mutant NMMHC-IIA can be expressed without abnormal aggregation in these cells remain to be elucidated, the differential expression of mutant NMMHC-IIA provides important insights into cell-specific regulation mechanisms in *MYH9* disorders. A comprehensive understanding of cell-specific NMMHC-IIA regulation will not only identify the hematologic abnormalities but also help to reveal the mechanisms of nonhematologic manifestations of *MYH9* disorders.

## Acknowledgments

We thank Drs T. Echizenya and M. Higashigawa for providing the patient samples, and Ms Y. Ito for skillful technical assistance.

This work was supported by grants to S.K. from the Japan Society for the Promotion of Science (nos. 16590971 and 18591094), the Ministry of Health, Labor and Welfare (Grant for Child Health and Development 19C-2), the Mother and Child Health Foundation, Charitable Trust Laboratory Medicine Foundation of Japan, and National Hospital Organization Research Fund.

## Authorship

Contribution: S.K. designed and performed research, analyzed data, and wrote the paper; M.H. analyzed data and wrote the paper; and H.S. supervised the research.

Conflict-of-interest disclosure: The authors declare no competing financial interests.

Correspondence: Shinji Kunishima, Department of Hemostasis and Thrombosis, Clinical Research Center, National Hospital Organization Nagoya Medical Center, 4-1-1 Sannomaru, Naka-ku, Nagoya 4600001, Japan; e-mail: kunishis@nnh.hosp.go.jp.

## References

- Hegglin R. Gleichzeitige konstitutionelle Veränderungen an Neutrophilen und Thrombocyten. *Helv Med Acta*. 1945;12:439-440.
- May R. Leukozyteneinschlüsse. *Dtsch Arch Klin Med*. 1909;96:1-6.
- Saito H, Kunishima S. Historical hematology: May-Hegglin anomaly. *Am J Hematol*. 2007 Nov 1; [Epub ahead of print].
- Kelley MJ, Jawien W, Ortel TL, Korczak JF. Mutation of *MYH9*, encoding non-muscle myosin heavy chain A, in May-Hegglin anomaly. *Nat Genet*. 2000;26:106-108.
- Kunishima S, Kojima T, Matsushita T, et al. Mutations in the NMMHC-A gene cause autosomal dominant macrothrombocytopenia with leukocyte inclusions (May-Hegglin anomaly/Sebastian syndrome). *Blood*. 2001;97:1147-1149.
- The May-Hegglin/Fechtner Syndrome Consortium. Mutations in *MYH9* result in the May-Hegglin anomaly, and Fechtner and Sebastian syndromes. *Nat Genet*. 2000;26:103-105.
- Dong F, Li S, Pujol-Moix N, et al. Genotype-phenotype correlation in *MYH9*-related thrombocytopenia. *Br J Haematol*. 2005;130:620-627.
- Heath KE, Campos-Barros A, Toren A, et al. Non-muscle myosin heavy chain IIA mutations define a spectrum of autosomal dominant macrothrombocytopenias: May-Hegglin anomaly and Fechtner, Sebastian, Epstein, and Alport-like syndromes. *Am J Hum Genet*. 2001;69:1033-1045.
- Kunishima S, Matsushita T, Kojima T, et al. Identification of six novel *MYH9* mutations and genotype-phenotype relationships in autosomal dominant macrothrombocytopenia with leukocyte inclusions. *J Hum Genet*. 2001;46:722-729.
- Seri M, Pecci A, Di Bari F, et al. *MYH9*-related disease: May-Hegglin anomaly, Sebastian syndrome, Fechtner syndrome, and Epstein syndrome are not distinct entities but represent a variable expression of a single illness. *Medicine (Baltimore)*. 2003;82:203-215.
- Kunishima S, Matsushita T, Kojima T, et al. Immunofluorescence analysis of neutrophil nonmuscle myosin heavy chain-A in *MYH9* disorders: association of subcellular localization with *MYH9* mutations. *Lab Invest*. 2003;83:115-122.
- Deutsch S, Rideau A, Bochaton-Piallat ML, et al. Asp1424Asn *MYH9* mutation results in an unstable protein responsible for the phenotypes in May-Hegglin anomaly/Fechtner syndrome. *Blood*. 2003;102:529-534.
- Pecci A, Canobbio I, Balduini A, et al. Pathogenic mechanisms of hematological abnormalities of patients with *MYH9* mutations. *Hum Mol Genet*. 2005;14:3169-3178.
- Jenis MEH, Takeuchi A, Dillon DE, Ruymann MFB, Rivkin S. The May-Hegglin anomaly: ultrastructure of the granulocytic inclusion. *Am J Clin Pathol*. 1971;55:187-196.
- Oski FA, Naiman JL, Allen DM, Diamond LK. Leukocytic inclusions-Dohle bodies-associated with platelet abnormality (the May-Hegglin anomaly): report of a family and review of the literature. *Blood*. 1962;20:657-667.

16. Volpe E, Cuccurullo L, Valente A, Jori GP, Buonanno G. The May-Hegglin anomaly: further studies on leukocyte inclusions and platelet ultrastructure. *Acta Haematol.* 1974;52:238-247.
17. Kunishima S, Matsushita T, Yoshihara T, et al. First description of somatic mosaicism in *MYH9* disorders. *Br J Haematol.* 2005;128:360-365.
18. Daniel JL, Sellers JR. Purification and characterization of platelet myosin. *Methods Enzymol.* 1992;215:78-88.
19. Imai Y, Matsushima Y, Sugimura T, Terada M. A simple and rapid method for generating a deletion by PCR. *Nucleic Acids Res.* 1991;19:2785.
20. Maupin P, Phillips CL, Adelstein RS, Pollard TD. Differential localization of myosin-II isozymes in human cultured cells and blood cells. *J Cell Sci.* 1994;107:3077-3090.
21. Pecci A, Noris P, Invernizzi R, et al. Immunocytochemistry for the heavy chain of the non-muscle myosin IIA as a diagnostic tool for *MYH9*-related disorders. *Br J Haematol.* 2002;117:164-167.
22. Sellers JR. Myosins: a diverse superfamily. *Biochim Biophys Acta.* 2000;1496:3-22.
23. Franke JD, Dong F, Rickoll WL, Kelley MJ, Kiehart DP. Rod mutations associated with *MYH9*-related disorders disrupt nonmuscle myosin-IIA assembly. *Blood.* 2005;105:161-169.
24. Cerecedo D, Stock R, Gonzalez S, Reyes E, Mondragon R. Modification of actin, myosin and tubulin distribution during cytoplasmic granule movements associated with platelet adhesion. *Haematologica.* 2002;87:1165-1176.
25. Tanaka K, Shibata N, Okamoto K, et al. Reorganization of myosin in surface-activated spreading platelets. *J Ultrastruct Mol Struct Res.* 1986;97:165-186.
26. White JG. Arrangements of actin filaments in the cytoskeleton of human platelets. *Am J Pathol.* 1984;117:207-217.
27. Jennings LK, Fox JE, Edwards HH, Phillips DR. Changes in the cytoskeletal structure of human platelets following thrombin activation. *J Biol Chem.* 1981;256:6927-6932.
28. Tanaka K, Itoh K. Reorganization of stress fiber-like structures in spreading platelets during surface activation. *J Struct Biol.* 1998;124:13-41.
29. Canobbio I, Noris P, Pecci A, Balduini A, Balduini CL, Torti M. Altered cytoskeleton organization in platelets from patients with *MYH9*-related disease. *J Thromb Haemost.* 2005;3:1026-1035.
30. Leon C, Eckly A, Hechler B, et al. Megakaryocyte-restricted *MYH9* inactivation dramatically affects hemostasis while preserving platelet aggregation and secretion. *Blood.* 2007;110:3183-3191.
31. Godwin HA, Ginsburg AD. May-Hegglin anomaly: a defect in megakaryocyte fragmentation? *Br J Haematol.* 1974;26:117-128.
32. Hamilton RW, Shaikh BS, Oattie JN, Storch AE, Saleem A, White JG. Platelet function, ultrastructure, and survival in the May-Hegglin anomaly. *Am J Clin Pathol.* 1980;74:663-668.
33. Chang Y, Aurade F, Larbret F, et al. Proplatelet formation is regulated by the Rho/ROCK pathway. *Blood.* 2007;109:4229-4236.
34. Chen Z, Naveiras O, Balduini A, et al. The May-Hegglin anomaly gene *MYH9* is a negative regulator of platelet biogenesis modulated by the Rho-ROCK pathway. *Blood.* 2007;110:171-179.
35. Schulze H, Shivdasani RA. Mechanisms of thrombopoiesis. *J Thromb Haemost.* 2005;3:1717-1724.
36. Matsushita T, Hayashi H, Kunishima S, et al. Targeted disruption of mouse ortholog of the human *MYH9* responsible for macrothrombocytopenia with different organ involvement: hematological, nephrological, and otological studies of heterozygous KO mice. *Biochem Biophys Res Commun.* 2004;325:1163-1171.
37. Mhatre AN, Li Y, Bhatia N, Wang KH, Atkin G, Lalwani AK. Generation and characterization of mice with *Myh9* deficiency. *Neuromolecular Med.* 2007;9:205-215.
38. Kunishima S, Yoshinari M, Nishio H, et al. Haematological characteristics of *MYH9* disorders due to *MYH9* R702 mutations. *Eur J Haematol.* 2007;78:220-226.
39. Fink L, Holschermann H, Kwapiszewska G, et al. Characterization of platelet-specific mRNA by real-time PCR after laser-assisted microdissection. *Thromb Haemost.* 2003;90:749-756.
40. Chung MC, Kawamoto S. IRF-2 is involved in up-regulation of nonmuscle myosin heavy chain II-A gene expression during phorbol ester-induced promyelocytic HL-60 differentiation. *J Biol Chem.* 2004;279:56042-56052.